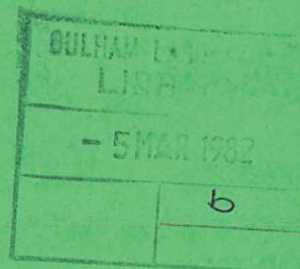




UKAEA

Preprint



COULOMB FRICTION IN MAGNETIC MULTIPOLE PLASMA SOURCES

A. J. T. HOLMES

CULHAM LABORATORY
Abingdon Oxfordshire

1981

This document is intended for publication in a journal or at a conference and is made available on the understanding that extracts or references will not be published prior to publication of the original, without the consent of the authors.

Enquiries about copyright and reproduction should be addressed to the Librarian, UKAEA, Culham Laboratory, Abingdon, Oxon. OX14 3DB, England.

COULOMB FRICTION IN MAGNETIC MULTIPOLE PLASMA SOURCES

A. J. T. Holmes

Euratom/UKAEA Fusion Association

Culham Laboratory, Abingdon, Oxon, U.K.

Abstract

A theoretical model of the effects of coulomb collisions between fast and thermal electrons in magnetic multipole or bucket plasma sources is described. The main effect of these collisions is to transfer energy from the ionising fast electrons to the plasma electrons and ions. This considerably reduces the ionisation rate in the discharge and at the same time raises the plasma electron temperature. Experimental measurements in a hydrogen discharge of both the ionisation rate and electron temperature have been made to test the theoretical model.

(Submitted for publication in Journal of Applied Physics)

September 1981

1. INTRODUCTION

It has been postulated by several authors^(1,2,3) that ionisation in ion sources based on arc discharges is due to primary electrons emitted from the cathode and accelerated across the cathode sheath. The thermal (low energy) electrons, arising from the slowing down of these primary electrons or from ionisation, are assumed to play no role in the ionisation process, although they may influence the break-up of molecular ions. However, at high densities the thermal electrons can provide an energy loss channel from the primaries and thereby decrease the ionisation efficiency of the source.

Here we examine the energy transfer process between primary electrons and plasma electrons by coulomb collisions and derive from this both the change in source ionisation efficiency and the change in plasma electron temperature arising from the energy transfer. The effects of beam-plasma interactions are neglected, as it is assumed that coulomb collisions are dominant, although it has been proposed that this process has some effect on the velocity distribution of the primaries⁽⁴⁾. The theoretical scaling of the ionisation rate and electron temperature that is obtained is compared with experiment.

2. ENERGY BALANCE OF THE PRIMARY ELECTRONS

Once the primary electron has attained its full energy by crossing the cathode sheath which has a thickness of a few debye lengths, it begins to lose energy via several loss processes. The dominant energy loss process is usually inelastic collisions which produce ion-electron pairs or excited molecules. In addition, the primary electron distribution can lose energy by coulomb friction, and also when some of the primaries strike the anode. The energy balance equation, representing the division of the input energy $I_p U_0$ into components, can be written:

$$I_p U_0 = H(U_0, n_0) + \int_0^{U_0} n_p f_p v m v \left(\frac{dv}{dt} \right)_c dU + \int_0^{U_0} e n_p f_p \frac{v A U}{4} dU \quad (1)$$

where n_0 is the gas density, v is the plasma volume, v is the primary velocity and U is its energy.

The first term represents the total power required to form all secondary particles including inelastic scattering and the initial kinetic energy given to secondary electrons. The second term is the coulomb friction, determined by $(dv/dt)_c$ for the normalised primary electron density distribution $n_p f_p(U)$. The last term is the anode loss where A represents the effective anode area.

The effective current of primaries to the anode, I_{pa} , is hence:

$$I_{pa} = \frac{1}{U_0} \int_0^{U_0} n_p f_p \frac{vA}{4} dU \quad (2)$$

Experimental measurements of the primary electron distribution have been made by Goede et al⁽⁵⁾. They have shown that $n_p f_p$ is essentially constant when U is less than U_0 , thus $n_p f_p$ can be removed from the integrands in equations 1 and 2. Each of the terms on the RHS of equation 1 can then be integrated as shown in the following sections.

2.1 The Inelastic Energy Loss

This loss can be derived from the average of all the collision rates and associated energy losses at a given energy and then integrating over the distribution function. However, during the ionisation process the secondary electrons receive a kinetic energy, ϕ , electron volts from the primary and also we assume that the primary retains an energy, ϕ , after it has been decelerated by inelastic collisions.

This assumption is justified as the quantum-mechanical wave functions of the two electrons emerging from an ionisation collision are indistinguishable. Hence the energy retained by a primary on average after it has ceased to have inelastic collisions cannot be different from other secondary electrons.

Hence:

$$\begin{aligned} H(U_0, n_0) &= \int_0^{U_0} n_p f_p n_0 \langle \sigma v \epsilon \rangle v dU + \phi [I_p - I_{pa} + I_+] \\ &= n_p f_p n_0 v \int_0^{U_0} \langle \sigma v \epsilon \rangle dU + \phi (I_p - I_{pa} + I_+) \end{aligned} \quad (3)$$

where $\langle \sigma v \epsilon \rangle$ is the average energy loss rate coefficient at energy U .

2.2 Coulomb Friction

Spitzer⁽⁶⁾ has shown that the slowing-down time, t_s , for a fast electron on an ion or electron maxwellian distribution, is:

$$\begin{aligned} t_{se} &= v v_e^2 / 2\Gamma n_e G(v/v_e) \\ t_{si} &= v v_i^2 / 2\Gamma n_e G(v/v_i) \end{aligned}$$

where $\Gamma = \frac{e^4 \ln \Lambda / 2}{\epsilon_0^2 m_e^2}$

and $v_e^2 = 2kT/m$

These expressions show that the slowing down time is long when the primaries are much faster than the plasma electrons or ions. However, this slowing down time on the plasma electrons only is reduced when the primaries have lost some of their initial energy. Thus, as the energy transfer is dominated by this shorter timescale, we can simplify the expressions for t_{se} and t_{si} to give:

$$t_{se} \approx v v_e^2 / 0.4 \Gamma n_e \quad (v \gg v_e)$$

$$t_{si} \approx 2v^3 / \Gamma n_e$$

The slowing down of the primary electrons through coulomb drag is thus given by:

$$\left(\frac{dv}{dt} \right)_c = v \left(\frac{1}{t_{se}} + \frac{1}{t_{si}} \right) = \Gamma n_e \left(\frac{0.4}{v_e^2} + \frac{1}{2v^2} \right)$$

The second term in equation (1) can now be integrated to yield:

$$\begin{aligned} \int_0^{U_0} n_p f_p v m v \left(\frac{dv}{dt} \right)_c dU &= n_p f_p m v \int_0^{U_0} v \Gamma n_e \left(\frac{0.4}{v_e^2} + \frac{1}{2v^2} \right) dU \\ &= n_p f_p v m \Gamma n_e \cdot \left(\frac{2e}{m} \right)^{1/2} \left[\frac{0.8 U_0^{3/2}}{3 v_e^2} + \frac{U_0^{1/2} m}{2e} \right] \end{aligned} \quad (4)$$

2.3 Anode Losses

The third term can be evaluated if the dependence of the effective anode area, A , on primary energy is known. Recent measurements⁽⁷⁾ on magnetic multipole sources have shown that:

$$A = \frac{\rho L}{V_z^{1/2}} U^{1/2}$$

where $\rho L / V_z^{1/2}$ is a coefficient based on the cusp length, L , and the anode magnetic field.

Hence
$$\int_0^{U_0} n_p f_p v \frac{AU}{4} dU = \rho L \frac{n_p f_p}{4 V_z^{1/2}} \cdot \left(\frac{2e}{m} \right)^{1/2} \cdot \frac{U_0^3}{3} \quad (5)$$

and

$$I_{pa} = \frac{\rho L n_p f_p}{4V_z^{1/2}} \frac{2e}{m} \frac{U_0^2}{2}$$

3. IONISATION EFFICIENCY

The total ion current, I_+ , produced in the discharge is given by:

$$I_+ = \int_{V_i}^{U_0} n_p f_p e v n_o \sigma_i v dU$$

To a good approximation the energy dependence of σ_i can be expressed by:

$$\sigma_i = \sigma_{io} (1 - v_i^2/U^2)$$

as demonstrated in Fig. 1, when a comparison is shown between this expression and the experimental value. Hence:

$$\begin{aligned} I_+ &= n_p f_p e v n_o \left(\frac{2e}{m}\right)^{1/2} \sigma_{io} \int_{V_i}^{U_0} (1 - v_i^2/U^2) \cdot U^{1/2} dU \\ &= n_p f_p e v_o n_o \sigma_{io} \left(\frac{2e}{m}\right)^{1/2} \left[\frac{2(U^{3/2} - v_i^{3/2})}{3} + 2v_i^2 (U_o^{-1/2} - v_i^{-1/2}) \right] \end{aligned}$$

If U_o exceeds twice V_i , then to a very good approximation:

$$I_+ = n_p f_p e v n_o \sigma_{io} \left(\frac{2e}{m}\right)^{1/2} \cdot \frac{2U_o^{3/2}}{3} \quad (6)$$

When equations 1, 2, 3, 4, 5 and 6 are combined, we find that:

$$\begin{aligned} \frac{I_p}{I_+} &= \frac{\phi}{U_o} \left[\frac{I_p}{I_+} + 1 - \frac{I_{pa}}{I_+} \right] + \int_0^{U_0} \langle \sigma v \epsilon \rangle dU \cdot [\sigma_{io} (2e/m)^{1/2} \cdot 2U_o^{5/2}/3]^{-1} \\ &\quad + \frac{\rho L U_o^{1/2}}{V_z^{1/2}} \cdot \frac{1}{8n_o v \sigma_{io}} + \frac{m \Gamma n_e}{n_o e \sigma_{io} U_o} \left[\frac{0.4}{v_e^2} + \frac{3m}{4eU_o} \right] \end{aligned}$$

Hence on simplifying we have:

$$\frac{I_p}{I_+} = \frac{1}{(U_0 - \phi)} \cdot \frac{3}{2U_0^{3/2} \cdot \sigma_{i0} \cdot (2e/m)^{1/2}} \cdot \int_0^{U_0} \langle \sigma v \epsilon \rangle dU$$

$$+ \frac{\rho L U_0^{1/2}}{V_z^{1/2}} \cdot \frac{1}{8n_0 v \sigma_{i0}} + \frac{S \beta I_+}{(U_0 - \phi) \cdot (kT/e)^{3/2}} \cdot \left[1 + \frac{7.5 m v_e^2}{4e U_0} \right] \quad (7)$$

$$\text{where } S = 0.2 \Gamma m_i^2 / A_s \alpha n_0 \sigma_{i0} e^{3.5}$$

The electron density, n_e , has been replaced by:

$$n_e = \beta I_+ / \alpha A_s e (kT/m_i)^{1/2}$$

where A_s is the ion collection area, β is the fraction of all ions going to this electrode and $\alpha (kT/m_i)^{1/2}$ is the ion sound speed.

This expression is equivalent to that developed by Green et al^(2,4) which is (in their notation):

$$\frac{I_p}{I_+} = \frac{\langle \sigma v \rangle_{IN}}{\langle \sigma v \rangle_{ION}} + \frac{1}{\tau_e \langle \sigma v \rangle_{ION} n_0}$$

The first and second terms in the above expression correspond to the first and second terms in equation 7, but the third term containing S arising from coulomb drag is new and will cause I_p/I_+ to increase with I_+ .

4. ENERGY BALANCE OF PLASMA ELECTRONS

Coulomb friction transfers energy from the primary electrons to the plasma electrons. In addition, there is the energy transfer during ionisation, ϕ . Hence the total input power is:

$$\phi(I_p - I_{pa} + I_+) + \int_0^{U_0} n_p f_p v m v \left(\frac{dv}{dt} \right)_c dU$$

$$= \phi(I_p - I_{pa} + I_+) + \frac{0.8 n_p f_p v m \Gamma n_e}{3 v_e} \left(\frac{2e}{m} \right)^{1/2} U_0^{3/2}$$

$$= \phi(I_p - I_{pa} + I_+) + \frac{0.4 n_e \Gamma m}{2 e v_e n_o \sigma_{io}} I_+ \quad (8)$$

The energy loss from the plasma electron distribution is the energy removed by the escape of plasma electrons and ions from the plasma and the energy transfer from the electrons of temperature T to the ions of temperature T_i ($T_i \ll T$). Harbour⁽⁸⁾ and Emmert et al⁽⁹⁾ have shown that for a negatively biased ion collector (i.e. several kT/e volts), the energy removed by the ions is 4 - 5 kT per ion. The energy removed by electrons is 2 kT per electron. Hence the total energy loss is:

$$\frac{kT}{e} [2(I_p - I_{pa} + I_+) + 4.5 I_+] + W_{ei} \quad (9)$$

where W_{ei} is the electron-ion energy transfer. Spitzer has shown that:

$$W_{ei} = \frac{n_e^2 v_{me} \ln \Lambda}{2 \epsilon_o (2 mkT)^{1/2} m_i} \text{ watts}$$

when $T \gg T_i$. Substitution of appropriate values shows that if $n_e \sim 10^{12} \text{ cm}^{-3}$ in a volume of 10^3 cm^3 for example, W_{ei} is about 2 watts, which is negligible in comparison with the other terms. However this energy is of significance in determining the ion temperature⁽¹⁰⁾.

If equations 8 and 9 are combined we have:

$$\phi \left(\frac{I_p}{I_+} - \frac{I_{pa}}{I_+} + 1 \right) + \frac{0.4 n_e \Gamma m^2}{2 e k T n_o \sigma_{io}} = \frac{kT}{e} \left(\frac{2I_p}{I_+} - \frac{2I_{pa}}{I_+} + 6.5 \right)$$

Hence simplification of the above equation yields:

$$\left(\frac{kT}{e} \right)^{3/2} \left(\frac{kT}{e} - \frac{kT_0}{e} \right) = S \beta I_+ / (6.5 + 2I_p/I_+ - 2I_{pa}/I_+) \quad (10)$$

$$\text{where } \frac{kT_0}{e} = \frac{\phi(I_p/I_+ - I_{pa}/I_+ + 1)}{(6.5 + 2I_p/I_+ - 2I_{pa}/I_+)}$$

Equation 7 also contains the term S , which is a measure of the energy lost by primary electrons through coulomb drag.

5. RESULTS

The plasma source used to make these measurements has been described elsewhere⁽⁷⁾. It is a magnetic multipole or bucket source which is capable of continuous operation up to 200 mA/cm². An outline drawing is shown in Fig.

2. This particular source operates with an apparent plasma potential which is more negative than the anode⁽⁷⁾. Thus the ions cannot reach the anode and hence can only strike the hot tungsten cathode or extraction electrode, which is biased more negatively than the cathode so that it collects only ions. As the cathode area is much smaller than the extraction electrode, β is close to unity and is estimated to be 0.9.

Data on the variation of βI_+ with I_p in a hydrogen discharge is shown in Fig.

3. It can be seen that $I_p/\beta I_+$ increases with βI_+ . Fig. 4 shows the dependence of T on βI_+ . T increases from an initial low value when βI_+ is almost zero and tends to a limiting value at high values of βI_+ . The variation of $I_p/\beta I_+$ with hydrogen gas pressure, p , is shown in Fig. 5, where a linear dependence with inverse pressure is observed. In this case p is derived from measurements with a baratron gauge in the absence of a discharge.

6. COMPARISON WITH THEORY

6.1 Electron Temperature Variations

The theory indicates an increase of T with I_p according to equation 10. To test this dependence we plot $(kT/e)^{3/2} (kT/e - kT_0/e)$ versus

$\beta I_+/(6.5 + 2I_p/\beta I_+)$. A set of straight lines in Fig. 6 are obtained whose theoretical slope is S_T where

$$S_T = 0.2 \Gamma m m_i^{1/2} / A_s \alpha \beta n_o \sigma_{io} e^{3.5}$$

(the T suffix indicates that this value is derived from electron temperature measurements). The abscissa is not quite the theoretical expression obtained in equation 10 as I_{pa} is not known. However, as this experiment has been performed at high gas densities, when the source has nearly its ultimate ionisation efficiency the error in neglecting I_{pa}/I_+ is small, particularly in comparison with the 6.5 term. The value of kT_0/e is derived from Fig. 4. The value of S_T and hence ϕ and also T_0 are shown in Table I.

Table I

U_o	S_T	ϕ	kT_o/e
60 V	$28(\text{eV})^{5/2} \text{ A}^{-1}$	10.4 eV	2.8 eV
100 "	62 "	11.1 "	2.55 "
120 "	108 "	10.3 "	2.2 "

6.2 Variation in Ionisation Efficiency

In Fig. 3, it can be seen that a set of straight lines is obtained when $I_p/\beta I_+$ is plotted as a function of βI_+ over the range of 8 to 25 A. The slope of these lines gives the value of S_I as shown in equation 7 (the I suffix indicates that S is obtained from ionisation efficiency data). Over most of this range kT/e is relatively constant as shown in Fig. 4, thus we can use this data to derive S_I . Values of S_I are listed in Table II together with appropriate values of S_T .

Table II

U_o	$d(I_p/\beta I_+)/d(\beta I_+)$	S_I	S_T
50 V	$6.5 \cdot 10^{-2} \text{ A}^{-1}$	-	-
60 "	$5.2 \cdot 10^{-2} \text{ A}^{-1}$	$28(\text{eV})^{5/2} \text{ A}^{-1}$	$28(\text{eV})^{5/2} \text{ A}^{-1}$
80 "	$3.7 \cdot 10^{-2} \text{ "}$	-	-
100 "	$4.2 \cdot 10^{-2} \text{ "}$	60 "	62 "
120 "	$4.8 \cdot 10^{-2} \text{ "}$	103 "	108 "

Very good agreement is obtained between the two values of S derived from different measurement techniques. This shows that the change in ionisation

efficiency caused by coulomb drag is directly related to the change in electron temperature.

6.3 Electron Loss to the Anode and Inelastic Losses

In Fig. 5, the dependence is shown of $I_p/\beta I_+$ on the reciprocal of the gas pressure (measured in the absence of a discharge with a baratron). A set of straight lines is obtained in agreement with the model (equation 7) at various arc voltages. These measurements have been made at a low value of βI_+ as can be seen by comparing Figs. 3 and 5.

The slope of $I_p/\beta I_+$ is theoretically proportional to $U_0^{1/2}$ as shown in equation 7. This slope is plotted against $U_0^{1/2}$ in Fig. 7 and a straight line is obtained in agreement with the theory. The slope of this line has the theoretical value of $\rho L/8V_z^{1/2} \beta v \sigma_{i0} K$ where K relates the gas density to the pressure. This slope determines the electron loss to the anode.

In Fig. 8 the intercept of $I_p/\beta I_+$ when $1/p$ is zero is plotted as a function of U_0 where a straight line is obtained. This suggests that:

$$\frac{2}{3} U_0^{3/2} \beta \sigma_{i0} \left(\frac{2e}{m}\right)^{1/2} \left[\int_0^{U_0} \langle \sigma v \epsilon \rangle dU \right]^{-1} = \frac{1}{59} \quad (\text{eV})^{-1}$$

$$\text{and } \phi = 13.5 \text{ eV}$$

The value of ϕ is in good agreement with the value derived in section 4.1 and the constancy of the integral equation above suggests that $\langle \sigma v \epsilon \rangle$ is not a function of U where:

$$\langle \sigma v \epsilon \rangle / \beta \sigma_{i0} = 59 \text{ eV}$$

7. DISCUSSION

The analysis of the experimental data above shows that the coefficients for the rate of change of temperature and ionisation (S_T and S_I) are identical and also the detailed scaling laws predicted by the model are in agreement with experiment. This agreement indicates that coulomb drag is the process which removes energy from the primary electrons, thereby reducing the ionisation rate, and hence heats the plasma electrons (and ions), which increases the electron temperature. The detailed fit to the experimental data requires that around 10 eV is transferred to an electron produced in an ionisation event, in agreement with calculations by Massey and Burhop⁽¹¹⁾, and a substantial fraction of this energy is lost from the plasma when the ions are accelerated

across the sheath of ion reflecting electrodes.

However, when the values of the constants incorporated in the value S are used to derive a theoretical value, we find that this value is between 4 and 16 times smaller than those values in Table II. This discrepancy may have two causes:

- (a) The calculation depends on the distribution function of the primary electrons. If f_p is other than uniform (as observed by Goede and Green) and had, for example, a dependence of $U^{(\delta-3/2)}$ then the coulomb drag would be enhanced by a factor of the order of $1/\delta$.
- (b) The value of S varies inversely as the gas density n_0 . At high discharge currents, Holmes and Green⁽¹²⁾ have shown that the power loadings in the ion extraction system attached to this plasma source require that the neutral gas density is lower by a factor of around 10 at high discharge currents.

We note that the variation of the electron temperature with discharge currents (Figs. 4 and 6) indicates that initially $(kT/e)^{3/2} (kT/e - kT_0/e)$ increases slowly and then more rapidly, thus giving an apparent intercept at a discharge current of around 5A. This could arise if the gas density is high at low currents, thus giving a low value of S . As the gas density diminishes, probably through discharge heating of the gas^(12,13), S increases and gives the steep dependence seen in Fig. 6. Further experiments to test this assumption are being planned.

Acknowledgement

The author would like to thank Dr. T. S. Green for his many helpful suggestions in the presentation of this paper.

References

- 1) C. Lejeune. Symp. Ion Sources, Brookhaven, BNL-50310, p.27, 1971.
- 2) T. S. Green, A. R. Martin, C. Goble and M. Inman. 7th European Conference on Controlled Fusion and Plasma Physics, p.93, Lausanne, 1975.
- 3) M. D. Gabovich. Sov. Phys. Tech. Phys., 12, p.638, 1967.
- 4) A. P. H. Goede and T. S. Green. Culham Report CLM P522 (1978). Also to be published in Phy. Fluids.
- 5) A. P. H. Goede, T. S. Green and B. Singh. J. App. Phys., 51, p.1896, (1980).
- 6) L. Spitzer. Physics of Fully Ionised Gases. (Interscience, New York, 1962).
- 7) A. J. T. Holmes. To be published in Rev. Sci. Instr.
- 8) P. J. Harbour. Culham Report CLM-P535, (1978).
- 9) G. A. Emmert, R. M. Wieland, A. T. Mense, and J. N. Davidson. Phys. Fluids, 23, p.803, 1980.
- 10) A. J. T. Holmes and M. Inman. Proc. of Linear Accelerator Conference, p.434, Brookhaven, 1979.
- 11) H. S. W. Massey and E. H. S. Burhop. Electronic and Ionic Impact Phenomena, 1, p.468, Oxford University Press, Oxford 1969.
- 12) A. J. T. Holmes and T. S. Green. Proc. 2nd Conference on Low Energy Ion Beams, p.163, Bath 1980.
- 13) F. Burrell, private communication.

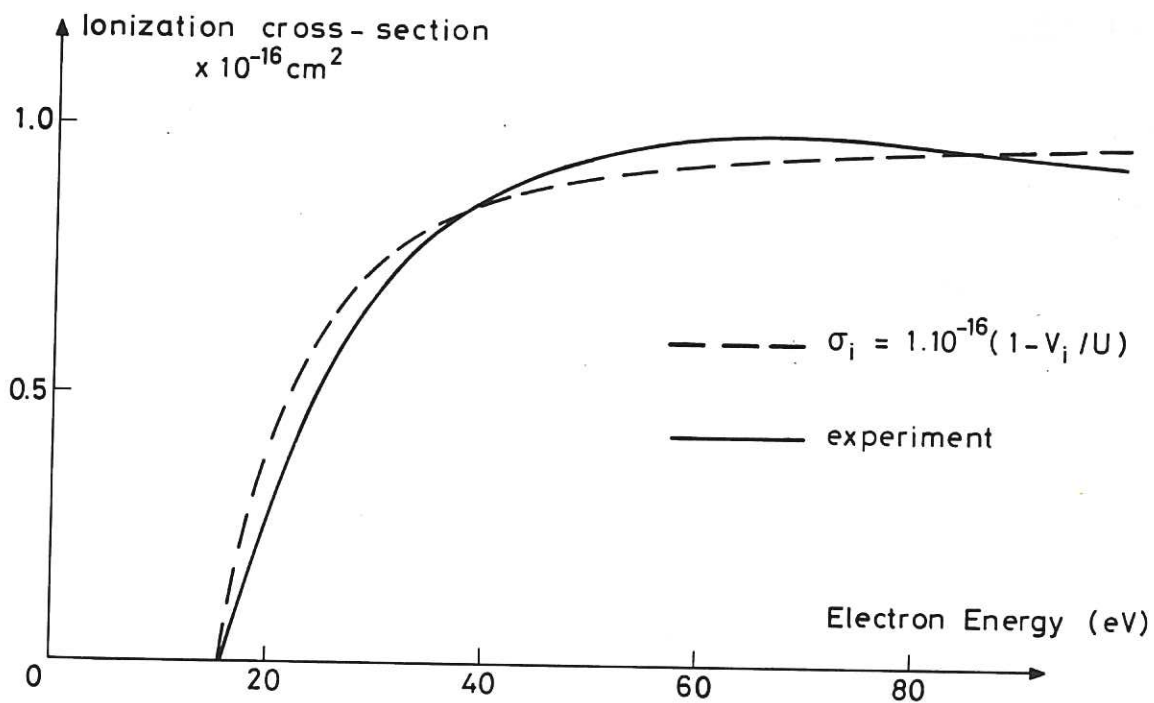


Fig.1 Comparison of the empirical energy dependence of the ionisation cross-section for H_2 with experimental measurements.

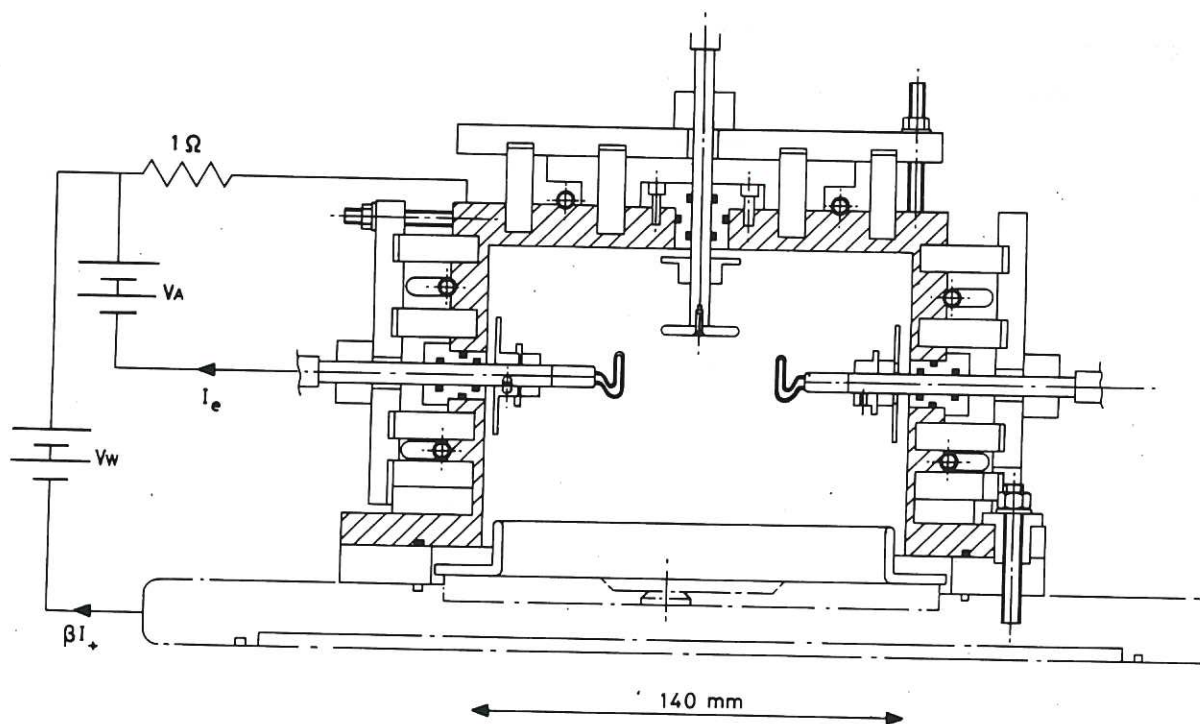


Fig.2 Cross-section view of the magnetic multipole or "bucket" source used to create the plasma in the experiment.

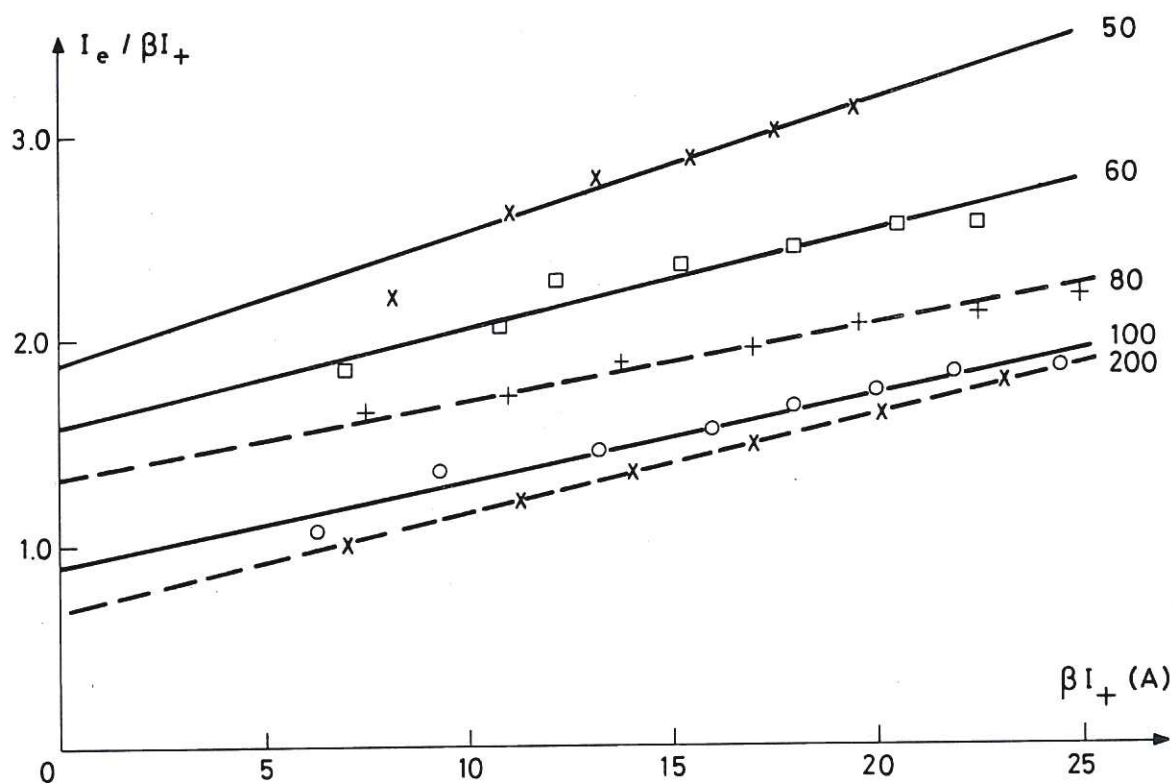


Fig.3 Variation of the ratio $I_e / \beta I_+$ with ion current or plasma density at a high hydrogen gas density in the discharge. The linear dependence is in agreement with Equation 7.

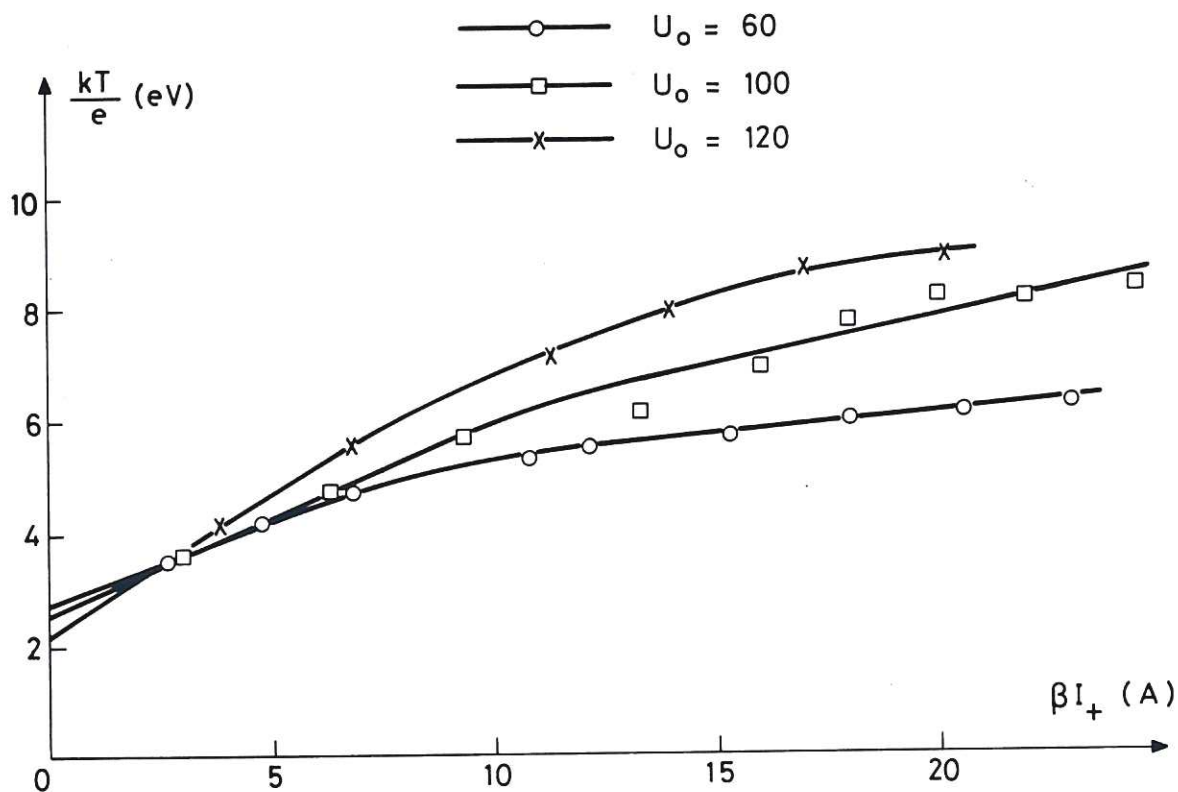


Fig.4 Dependence of the electron temperature on the ion current. The temperature tends to a limiting value at high discharge powers.

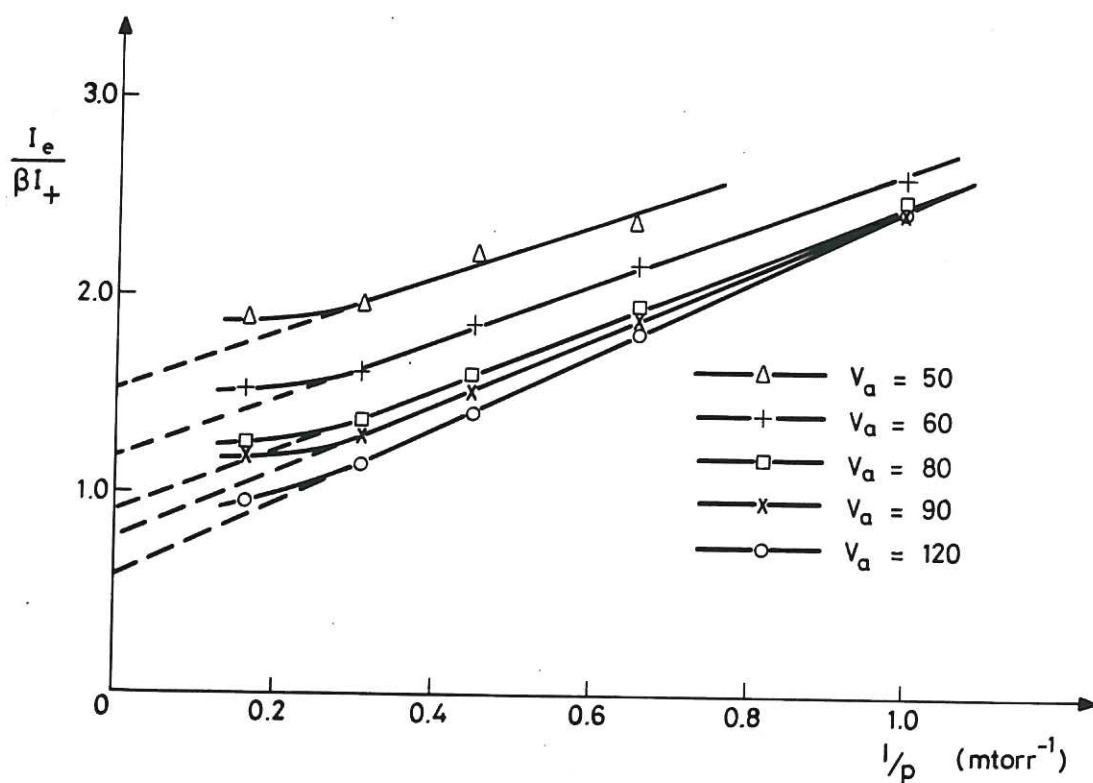


Fig.5 Variation of the ratio of $I_p/\beta I_+$ with the reciprocal of the gas pressure. The pressure is measured with a baratron gauge in the absence of a discharge.

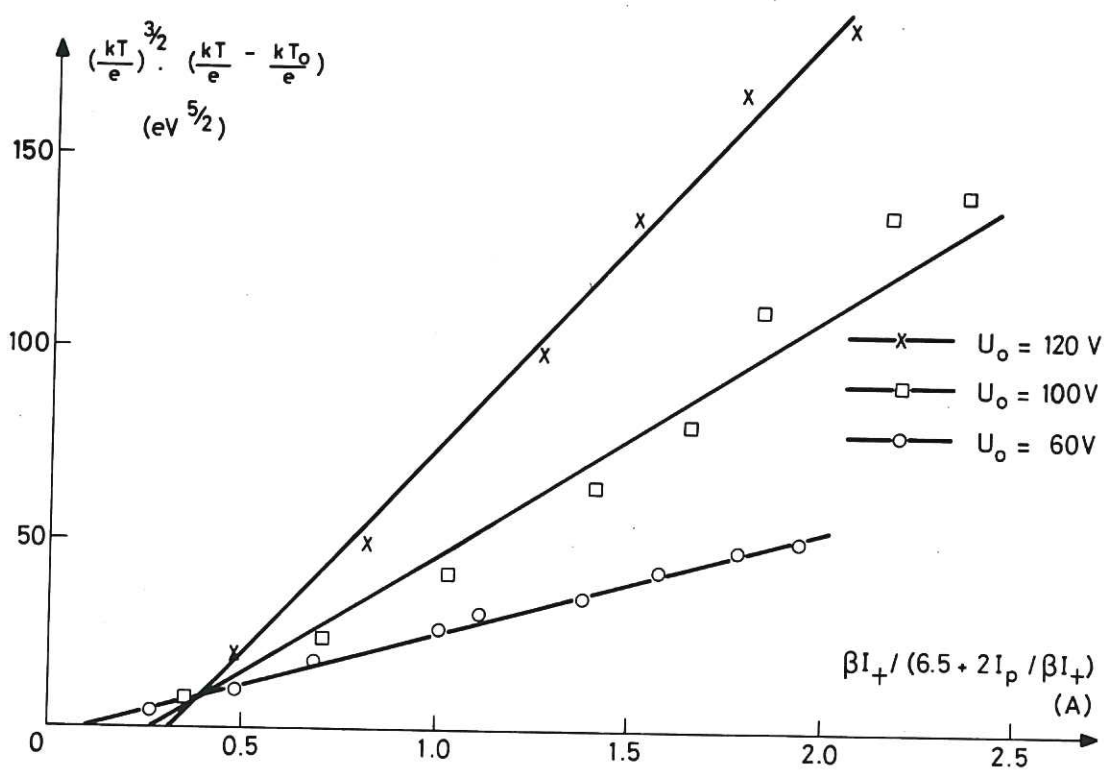


Fig.6 The dependence of the electron temperature on ion current when plotted according to the predictions of Equation 10. The straight lines obtained indicate that this equation is obeyed.

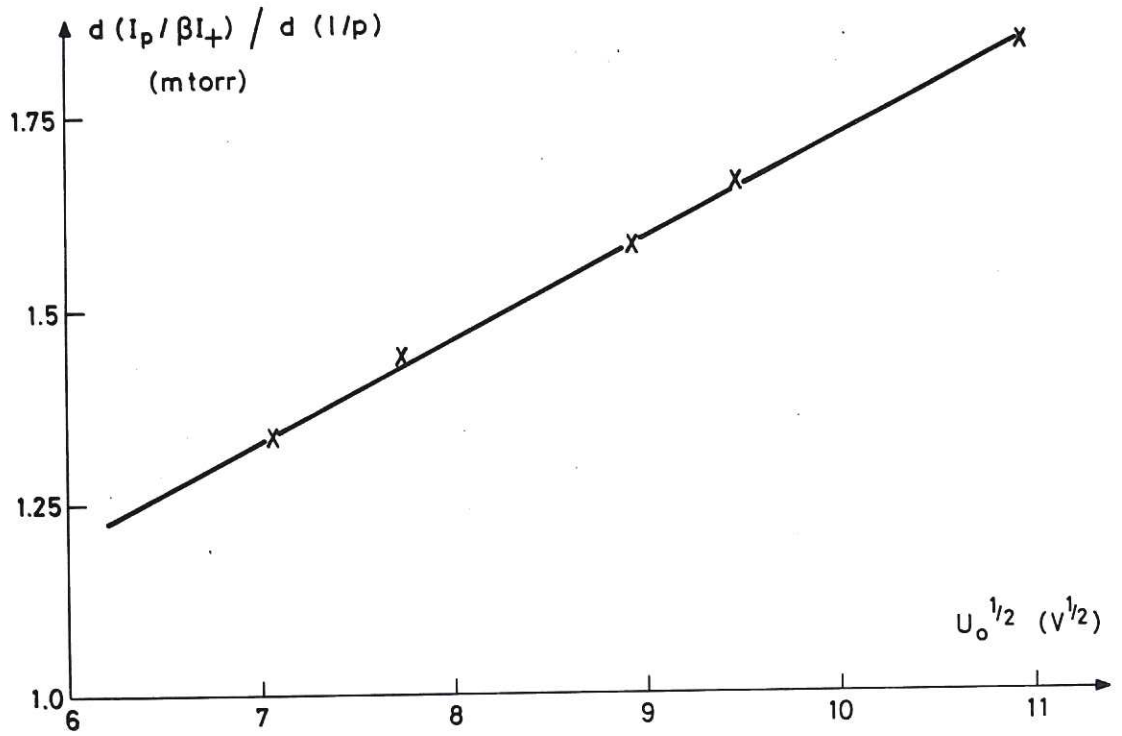


Fig.7 The slope of the lines in Fig.5 are plotted as a function of $U_o^{1/2}$ yield a straight line which is in agreement with Equation 7.

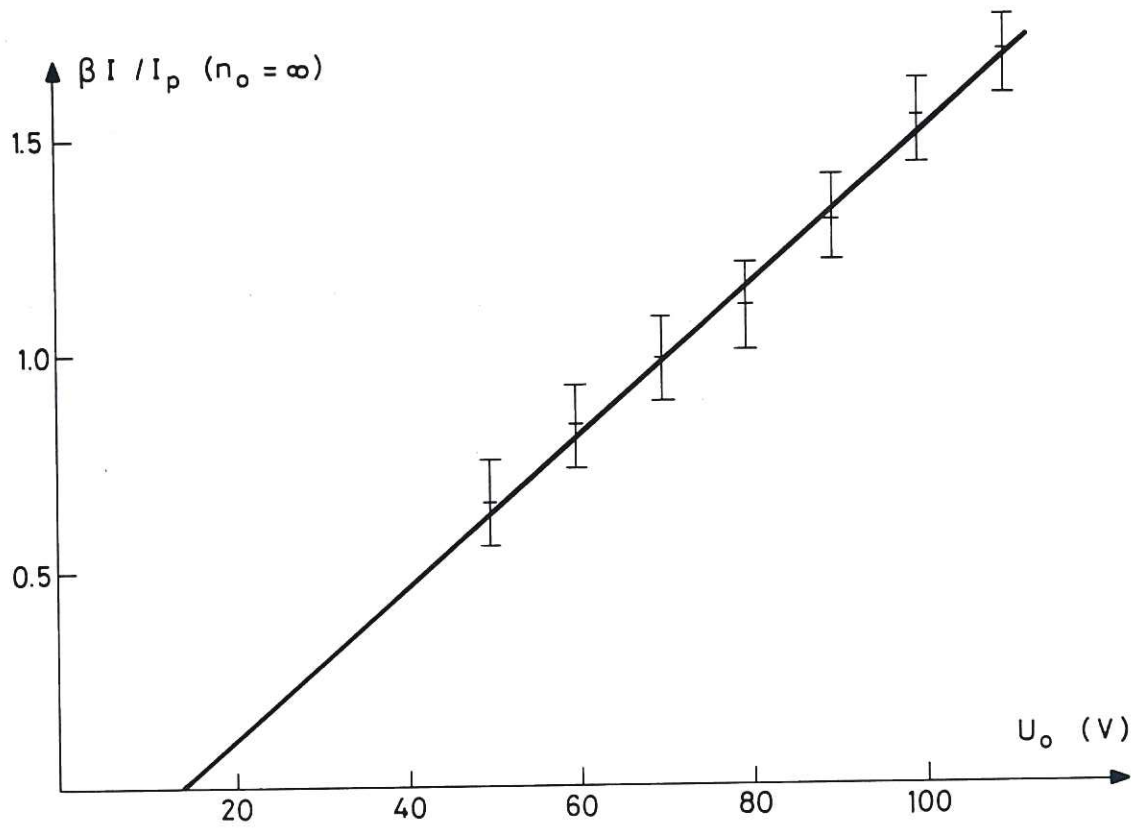


Fig.8 The intercepts of the lines in Fig.5 on the $I_p / \beta I_+$ axis are plotted as a function of U_o . The slope of this line is the reciprocal of the overall energy required to create an ion in the source.



